Optimal paths for thermodynamic systems: The ideal diesel cycle

Karl Heinz Hoffman,[a] Stanley J. Watowich, and R. Stephen Berry
Department of Chemistry and the James Franck Institute, The University of Chicago, Chicago, Illinois 60637

(Received 4 March 1985; accepted for publication 15 May 1985)

Optimal control theory is used to determine the piston trajectory which yields maximum power output for a model which incorporates the diesel engine's major irreversibilities. Optimal trajectories were obtained for the cases of unconstrained and constrained piston acceleration. Optimizing the path for our standard engine increased both the net work output per cycle and the net efficiency by about 10%.

I. INTRODUCTION

While traditional thermodynamics of equilibrium systems provides rigorous bounds on the possible performance of real processes, these bounds are often far from what can be obtained by real processes operating in finite times or at nonzero rates. By including time- and rate-dependent terms in the system analysis it is possible to determine more realistic bounds on process performance. Such an analysis also elucidates how bounds on process performance are governed by the operating rate of the system and can lead to the construction of the path or paths which yield extremal process performance.

Our analysis, based on the above goals, has three characteristics that distinguish it from equilibrium thermodynamics and engineering design: (1) the objects of the analysis are ordinarily simplified abstractions of real systems, much as the air-standard cycles are simplified abstractions for conventional thermodynamics, so that computations are simpler and far more economical than computations for very detailed, realistic models. (2) The inclusion into the models of the main sources of dissipation leads to bounds on performance more realistic and more useful than bounds based on reversible processes. (3) The relative importance of different loss terms can be compared so that the most effective directions for further improvements can be selected.

Previous work has dealt with heat engines modeled with finite heat-conduction rates between heat reservoirs and the working fluid[1–6] and with friction.[6,7] These works determined piston trajectories which optimized efficiency, entropy production, power, and/or net revenue. In this paper we find the piston path yielding maximum power for an idealized diesel engine with friction, heat leak and a finite combustion rate. Including a time-dependent heating function in our model extends this work to a much wider class of processes than had been discussed previously. We also consider how bounds on the piston's acceleration and deceleration affect the optimal trajectory and the engine's performance. This allows us to include cases where piston masses and forces are finite.

II. DESCRIPTION OF THE MODEL

The model can be viewed either as a simplified diesel engine or as a dual combustion "air-standard" cycle with rate-dependent loss mechanisms. The model's piston motion is based on a four-stroke cycle of successive intake, compression, power and exhaust strokes. Cycle period, fuel intake per cycle, fuel-air mixture composition, and compression ratio are taken as constant. The piston's path is the time-parametrized function chosen to optimize power output.

Section II A describes the functions modeling the combustion reaction within the diesel engine. Section II B describes the major loss terms included in our model. Section II C briefly reviews conventional piston paths for real diesel engines.

A. Finite combustion rate

In the diesel engine, fuel is injected towards the end of the compression stroke. Following injection there is commonly a delay before sufficient fuel evaporates and burns to initiate a noticeable rise in temperature and pressure. Part of the injected fuel is burned rapidly and early during the power stroke. The remaining fuel burns relatively slowly as it evaporates and diffuses into oxygen-rich regions where combustion can be sustained. In moderately and heavily loaded engines, this burning continues for most of the power stroke.

Our model assumes that injection is timed so that the temperature rise begins at minimum volume. The finite rate of the combustion process is approximated by the following time-dependent function which describes the extent of the reaction

$$\mathrm{Rn}(t) = F + (1 - F)[1 - \exp(-t/t_b)]. \tag{1}$$

The explosion fraction F is the fraction of the fuel charge consumed in the initial instantaneous burn, and t_b is the relaxation or burn time during which most of the combustion occurs. For the corresponding heating function $h(t)$, we take

$$h(t) = Q_c \dot{\mathrm{Rn}}(t) \tag{2}$$

where Q_c is the heat of combustion per molar fuel-air mixture charge. We assume that Q_c is temperature independent. The dot notation signifies the time derivative $d(\,)/dt$ in the usual way.

The mole number N and heat capacity C are assumed to be influenced by the extent of the combustion reaction within the piston chamber. We express this dependence as

$$N = N(t) = N_i + (N_f - N_i)\mathrm{Rn}(t) \tag{3a}$$

and

$$C = C(t) = C_i + (C_f - C_i)\mathrm{Rn}(t). \tag{3b}$$

[a] Institute for Theoretical Physics, University of Heidelberg, D6900 Heidelberg, Federal Republic of Germany.

 0021-8979/85/182125-10$02.40

The subscripts i and f refer to conditions at $\mathrm{Rn} = 0$ and $\mathrm{Rn} = 1$, respectively. We further assume that the heat capacities of the reactants and products are temperature independent.

B. Loss terms

Conventional "air-standard" cycles which traditionally serve as idealized models of operating diesel engines neglect losses due to irreversible, time-related phenomena. For the diesel cycle the main losses are as follows[8]: (1) friction, (2) pressure drop, (3) heat leak, (4) fuel injection, (5) incomplete combustion, and (6) exhaust blowdown. The non-negligible losses from this list are cast into simplified functional forms and incorporated into our model. This approach reproduces the diesel engine's salient features in a flexible, easily decipherable model.

1. Friction loss

Frictional forces are assumed proportional to the piston velocity v.[9] The frictional work W_f in time t, is expressed as

$$W_f = \int_0^t \alpha v^2 dt. \tag{4}$$

This form corresponds to a well-lubricated sliding surface.

Owing to the greater pressure on the piston during the power stroke, the mechanical friction term α is roughly twice as large in the power stroke as it is in the other strokes.[10] On all strokes the sliding friction coefficient is assumed constant.

Heat generated by frictional work is removed by the engine's cooling system. We will not discuss possible enhancements of performance based on using this energy as a low-grade heat source.

2. Pressure drop

Each fresh charge of air is provided by opening the intake valve at the beginning of the intake stroke. Withdrawal of the piston creates a pressure differential between the environment and the piston chamber that draws in air. Viscous flow through the constricted intake generates a velocity-dependent force which opposes piston motion. In our model this force is treated as a frictionlike loss term with a magnitude twice that of the previously described sliding friction coefficient.[7] On the intake stroke the combined effects of sliding friction and viscous forces are represented by setting the friction coefficient in Eq. (4) to 3α.

Similar losses do not occur on the exhaust stroke. This is discussed further in the exhaust blowdown section.

3. Heat leak

We assume a Newton-type heat leak proportional to the exposed interior area of the piston cylinder and to the difference between the temperatures of the working fluid and the cylinder walls. With the piston at position x, the heat leak is given by

$$\dot{Q} = k\pi b\,(0.5b + x)(T_w - T), \tag{5}$$

where k is the cylinder's heat transfer coefficient, b is the cylinder's diameter or bore, and T_w is the temperature of the cylinder wall. These design parameters are time independent. Since the average value of $T_w - T$ is small along the nonpower strokes we assume the heat leak losses along these strokes are negligible.

4. Fuel injection

We assume that negligible work is expended in injecting the liquid fuel charge into the cylinder. Also assumed negligible are the temperature and pressure changes immediately following fuel injection.

5. Incomplete combustion

If the exhaust valve opens before the burning fuel-air mixture reaches chemical equilibrium there can be minor efficiency losses even in well-adjusted engines operating at normal loads. We include these losses in our model by representing the combustion reaction as the exponential function given explicitly in Eq. (1).

6. Exhaust blowdown loss

To avoid pressure losses during the exhaust stroke the exhaust valve is commonly opened before the power stroke is completed. The relatively high pressures at this point purge the cylinder of residual gases. This practice is estimated to result in work output losses of 2%.[11] This loss is not included in our model.

C. Conventional piston path

To determine improvements resulting from the optimized piston motion, power output and engine efficiencies are calculated for conventional piston trajectories. Piston motion within a conventional diesel engine may be described by

$$\dot{x} = 2\pi\Delta x \sin(\theta)/\tau\{1 + (r/l)\cos(\theta) \times [1 - (r/l)^2\sin(\theta)^2]^{0.5}\}. \tag{6}$$

As seen in Fig. 1, x denotes piston position, $\Delta x = 2r$, and

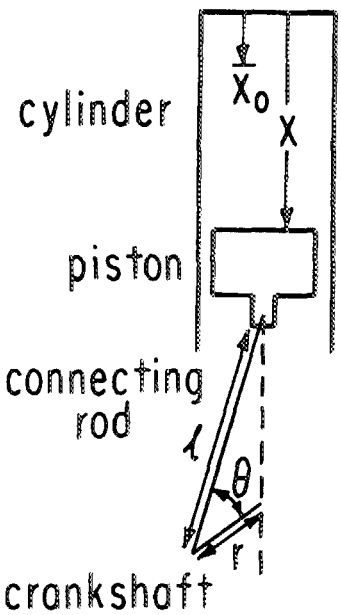

FIG. 1. Conventional piston linkage.

$\theta = 4\pi t/\tau$. At time $t = 0$ we assume $x = x_0$. The four-stroke cycle period is τ. Pure sinusoidal piston motion occurs when $\lim_{l\to\infty} r/l = 0$. In our work we set $r/l = 0.25$, as in Ref. 7.

The engine parameters described above are assigned values in Table I. These values are adapted from Taylor[8] and are chosen to be compatible with the parameters used in Mozurkewich and Berry's work.[7]

III. OPTIMIZATION PROCEDURE

We wish to maximize the power output from our generic model of the diesel engine. We use as a control function the piston's time path. Since fuel input and cycle time are fixed, the path yielding maximum power simultaneously maximizes thermodynamic engine efficiency and work output per cycle.

The optimization is viewed as a six-step process. Steps (1)–(3) determine the piston path which minimizes frictional losses along the compression, intake, and exhaust strokes, respectively. Step (4) allocates a fixed time among the nonpower strokes to minimize frictional losses during the three nonpower strokes. Note that in the nonpower strokes minimizing frictional losses is equivalent to maximizing the work output. Step (5) determines the piston trajectory which maximizes work output along the power stroke. Step (6) allocates the fixed cycle time between the nonpower and power strokes to maximize net work output over the entire cycle.

Optimal control theory[12,13] is used in steps (1)–(3) and (5) to determine the piston trajectories. The expressions for the nonpower strokes are straightforward and are solved analytically in steps (1)–(3). This calculation serves as a preview to step (5), where the determination of the optimal trajectory is not transparent.

Constraints on the trajectory naturally restrict the form of the optimal path. This makes it convenient to treat unbounded and bounded acceleration as distinct cases of the same model. Unbounded and bounded acceleration are discussed in the remainder of this paper under the subsection headings *1* and *2*, respectively.

TABLE I. Engine parameters. Parameters based on data from Refs. 7 and 8.

Mechanical parameters
compression ratio: 16
$x_0 = 0.5$ cm, $x_f = 8.0$ cm
cylinder bore $b = 7.98$ cm
cylinder volume $V = 400$ cm
cycle time $\tau = 33.33$ msec corresponding to 3600 rpm
Thermodynamic parameters
initial temperature, compression stroke: 329 K
number of moles of gas $N_i = 0.0144$
$N_f = 0.0157$
constant-volume heat capacity $C_i = 2.5\,R$
$C_f = 3.35\,R$
cylinder wall temperature $T_w = 600$ K
Loss term coefficients
friction coefficient $\alpha = 12.9$ kg sec^{-1}
heat-transfer coefficient $k = 1305$ kg K^{-1} sec^{-3}
Heat function parameters
explosion fraction $F = 0.5$
burn time $t_b = 2.5$ msec
heat of combustion $Q_c = 5.75\times10^4$ J per molar fuel-air mixture charge
Gas constant $R = 8.3144$ J K^{-1} mol^{-1}

A. Steps (1)–(3): Nonpower stroke trajectory

Frictional losses along the compression, intake, and exhaust strokes are minimized. For brevity we discuss this minimization for a general nonpower stroke i. From Eq. (4) the friction loss for stroke i, completed in time t_i, is

$$W_{fi} = \int_0^{t_i} \alpha_i v_i^2 dt. \tag{7}$$

1. Nonpower strokes with arbitrary acceleration

For unbounded acceleration the sole constraint on piston motion is

$$\dot{x}_i = v_i. \tag{8}$$

The Hamiltonian for this simple system is

$$H = -\alpha_i v_i^2 + \lambda v_i. \tag{9}$$

The canonical equation for λ, conjugate to the state variable x_i, is

$$\dot{\lambda} = -\frac{\partial H}{\partial x_i} = 0. \tag{10}$$

The Pontryagin maximum principle requires H to be maximized with respect to v_i. Solving $\partial H/\partial v_i = 0$ yields

$$v_i = \lambda/(2\alpha_i) = \text{const} \tag{11}$$

as the trajectory which maximizes H, provided this solution is not a boundary solution.

Since the boundary conditions on the piston's position are

$$x_i(0) = x_{i0} \tag{12a}$$

and

$$x_i(t_i) = x_{if} \tag{12b}$$

we rewrite equation (11) as

$$v_i = (x_{if} - x_{i0})/t_i = \Delta x_i/t_i, \tag{13}$$

which is a perfectly satisfactory interior extremum for H.

2. Nonpower strokes with bounded acceleration

We now limit the piston's acceleration, adding the differential constraint

$$\dot{v}_i = a_i. \tag{14}$$

The acceleration a_i must satisfy the inequality constraints $-a_{\max} \leqslant a_i \leqslant a_{\max}$. Initial and final piston velocities are chosen to be zero.

From Eqs. (7), (8), and (14) we form the Hamiltonian

$$H = -\alpha_i v_i^2 + \lambda_1 v_i + \lambda_2 a_i. \tag{15}$$

The Hamiltonian, linear in the control variable, is maximized by

$$a_i = \begin{cases} -a_{\max} & \text{when} \quad \lambda_2 < 0 \\ a_{\max} & \text{when} \quad \lambda_2 > 0 \\ \text{indeterminate} & \text{when} \quad \lambda_2 = 0. \end{cases} \tag{16}$$

When $\lambda_2 = 0$ the equations governing the optimal arc mimic those derived for the case of unconstrained acceleration.

The optimal trajectory for the constrained acceleration case follows a three-branch path: (a) From an initial velocity of zero the piston accelerates at the maximum rate $a_{\max}$. (b) At time t' the motion switches to the constant velocity arc described by Eq. (11). The piston moves along this arc with velocity $a_{\max}\, t'$ until time $t_i - t'$. (c) Then the piston motion switches to the arc governed by $a_i = -a_{\max}$. The piston moves along this arc until its velocity is zero.

Since the piston travels the distance Δx_i in time t_i, we find the time t' spent on each bounded acceleration arc by solving

$$\Delta x_i = a_{\max} t'^2 + a_{\max}(t_i - 2t'). \tag{17}$$

This gives

$$t' = 0.5 t_i (1 - y_i), \tag{18}$$

where

$$y_i = [1 - 4\Delta x_i/(a_{\max} t_i^2)]^{0.5}. \tag{19}$$

B. Step (4): Allocation of time along the nonpower strokes

The path determined in steps (1)–(3) for nonpower stroke i has a friction loss of

$$W_{if} = \tfrac{1}{12}\alpha_i a_{\max}^2 t_i^3 (1 + 2y_i)(1 - y_i)^2. \tag{20}$$

We define the time spent on all three nonpower strokes as t_{NP} and allocate t_{NP} among the compression, intake, and exhaust strokes to minimize total frictional losses along these strokes.

The friction coefficients for the compression, intake, and exhaust strokes were assumed α, 3α, and α, respectively. Since friction loss is identical along the compression and exhaust strokes, the time t_1 allocated to these strokes is identical. Call the time allocated to the intake stroke t_2. The frictional loss on these three nonpower strokes is

$$W_f = \sum_i W_{if} = \tfrac{1}{6}\alpha a_{\max}^2 [t_1^3 (1 - y_1)^2 (1 + 2y_1) + \tfrac{3}{2} t_2^3 (1 - y_2)^2 (1 + 2y_2)]. \tag{21}$$

With $t_{NP} = 2t_1 + t_2$ as a constraint, minimization of

$$W_f + \lambda (2t_1 + t_2)$$

yields the relation

$$t_1^2 (1 - y_1)^2 = 3 t_2^2 (1 - y_2)^2. \tag{22}$$

Equation (22) is solved numerically for given values of t_{NP}.

C. Step (5): Trajectory for the power stroke

We wish to maximize the work output of the power stroke. Work output, in time t_P, is expressed by the integral

$$W_P = \int_0^{t_P} (NRT v/x - \alpha v^2) dt. \tag{23}$$

1. Power stroke with arbitrary acceleration

With unlimited acceleration piston velocity is again the control variable. The temperature and position state variables, T and x, respectively, are subject to the constraints

$$\dot{T} = -(NC)^{-1}[NRT v/x + k\pi b \times (b/2 + x)(T - T_w) - h(t)] \tag{24}$$

and

$$\dot{x} = v, \tag{25}$$

where the heating is related to the heat of combustion and burn time t_b by

$$h(t) = Q_c (1 - F)(1/t_b)\exp(-t/t_b), \tag{26}$$

as noted in Eq. (2). Mole number N and heat capacity C are functions of the reaction coordinate Rn(t), as given by equations (3a) and (3b). The Hamiltonian for this problem is

$$H = NRT v/x - \alpha v^2 - \lambda_1 (NC)^{-1}[NRT v/x + k\pi b (b/2 + x)(T - T_w) - h(t)] + \lambda_2 v. \tag{27}$$

The adjoint variables are the solutions of

$$\dot{\lambda}_1 = -\frac{\partial H}{\partial T} = NR \quad v/x[\lambda_1 (NC)^{-1} - 1] + (\lambda_1/NC) k\pi b (b/2 + x) \tag{28}$$

and

$$\dot{\lambda}_2 = -\frac{\partial H}{\partial x} = NRT v/x^2 [1 - \lambda_1 (NC)^{-1}] + \lambda_1 (NC)^1 k\pi b (T - T_w). \tag{29}$$

Maximizing the Hamiltonian by setting $\partial H/\partial v = 0$ yields

$$v = (1/2\alpha)\{\lambda_2 + (NRT/x)[1 - \lambda_1 (NC)^{-1}]\}. \tag{30}$$

The boundary conditions for the system of equations (24), (25), (28) and (29) are

$$T(0) = T_0, \tag{31a}$$

$$x(0) = x_0, \tag{31b}$$

$$x(t_P) = x_f, \tag{31c}$$

and

$$\lambda_1(t_P) = 0. \tag{31d}$$

Equation (31d) results from allowing the end temperature to be unconstrained.

Numerical solutions to this control problem were carried out on a VAX 11/780. This system of four coupled ordinary differential equations was integrated with an initial-value differential equation solver. The unknown values, $\lambda_1(0)$ and $\lambda_2(0)$, were initially guessed. The resultant values of $x(t_P)$ and $\lambda_1(t_P)$ were compared with the desired boundary conditions, equations (31c) and (31d). The guessed initial values were then modified to minimize the square of the deviation between the resultant and desired final values. A multivariable, multiconstrained function-optimizing routine, VMCON,[14] provided an efficient method for performing this minimization.

The constraint that the minimum volume occurs when the piston position is x_0 gives rise to a boundary arc of $x \geqslant x_0$. Without this boundary constraint the above system yields a path that initially drops x below x_0. With the piston position constraint we thus anticipate a two-branch path. The control variable along this path is

$$v(t) = 0 \quad \text{for } 0 \leqslant t \leqslant t_d \tag{32}$$

and

$$v(t) = (1/2\alpha)\{\lambda_2 + (NRT/x)[1 - \lambda_1 (NC)^1]\}$$

for $t_d \leqslant t \leqslant t_P$.

The differential equation solver determines t_d, the motion delay time, in the following manner: For each iteration along the independent variable t the velocity $v(t)$ is set equal to 0 if the condition $x(t) \geqslant x_0$ would be violated. This determines the time interval from $t = 0$ to $t = t_d$.

2. Power stroke with bounded acceleration

We modify the above problem by constraining piston acceleration. Our goal remains the maximization of the objective function given by Eq. (23), but the control variable is now the acceleration a. The differential constraints on the state variables T and x remain as given in Eqs. (24) and (25), respectively. Explicit dependence on acceleration is introduced by the constraint equation

$$\dot{v} = a. \tag{33}$$

The acceleration is subject to the inequality constraints of

$$-a_{\max} \leqslant a \leqslant a_{\max}. \tag{34}$$

The Hamiltonian is now

$$\begin{aligned} H = {} & NRTv/x - \alpha v^2 - (\lambda_1/NC) \\ & \times [NRTv/x + k\pi b(b/2 + x)(T - T_w) - h(t)] \\ & + \lambda_2 v + \lambda_3 a, \end{aligned} \tag{35}$$

where

$$h(t) = Q_c(1 - F)(1/t_b)\exp(-t/t_b). \tag{36}$$

The canonical equations conjugate to T and x are expressed by Eqs. (28) and (29), respectively. The adjoint variable for Eq. (33) is

$$\dot{\lambda}_3 = -\frac{\partial H}{\partial v} = 2\alpha v - \lambda_2 - (NRT/x)(1 - \lambda_1/NC). \tag{37}$$

Boundary conditions for this system of coupled differential equations are given both by Eqs. (31) and by the requirement that piston velocity be zero at both end points of the path.

The Hamiltonian is linear in the control variable. Maximizing H requires

$$a = \begin{cases} a_{\max} & \text{when } \lambda_3 > 0 \\ -a_{\max} & \text{when } \lambda_3 < 0. \end{cases} \tag{38}$$

When $\lambda_3 = 0$, the Hamiltonian reduces to Eq. (27) and the value of a no longer enters explicitly into the maximization of H. If $\lambda_3 = 0$ for the interval $[t_d, t']$, subject to $0 \leqslant t_d \leqslant t' < t_P$, then obviously

$$\dot{\lambda}_3 = 0 \tag{39}$$

inside this interval. Solving Eqs. (37) and (39) yields the velocity as a function of the remaining state and adjoint variables. This expression, not surprisingly, is identical to Eq. (30).

The optimal trajectory with bounded acceleration is a three-branch path: (a) From the initial time $t = 0$ to the motion delay time $t = t_d$ the piston remains along a zero velocity arc at the initial position x_0. (b) Beginning at time $t = t_d$ the piston follows an interior arc described by the unconstrained acceleration path given by Eq. (30). (c) At $t = t'$ the trajectory switches to the arc given by $a = -a_{\max}$. The piston moves along this final arc until time $t = t_P$, at which time the piston velocity reaches zero.

D. Step (6): Maximization of the net work

Net work output

$$W(\tau) = W_P(t_P) - W_f(t_{\mathrm{NP}}) \tag{40}$$

was maximized for the entire cycle during this step. The total cycle time τ is a fixed engine parameter, but must be allocated between t_N and t_{NP}.

The maximization of Eq. (40) was accomplished numerically by a line search, varying t_P and comparing resulting values of $W(\tau)$. The computational efficiency was increased by predicting the initial values of the adjoint variables from a quadratic fit of the results of the preceding three runs of the line search.

IV. RESULTS

A. Sets of parameters

Piston trajectories which maximize net work output (hence called optimal piston trajectories or paths) were calculated for engines with the parameters listed in Tables I and II. The standard reference engine, labeled "case Std," corresponds to the parameter values listed in Table I. Variations of case Std are given in Table II.

Optimized piston trajectories were obtained for both unconstrained and constrained acceleration limits for all but one parameter set. Optimal trajectories were obtained for only the unconstrained acceleration limits for case I. The bound on acceleration, when imposed, is 3 cm/msec^2. This limit is mechanically feasible, being roughly the maximum acceleration reached in conventional automobile diesel engines.[15] This limit also illustrates the point that the improvements in power and efficiency are quite similar, whether they are obtained by optimizing unbounded or bounded acceleration limits. Finally, the acceleration on the second arc of the power stroke of the optimal path with bounded acceleration remains less than the 3-cm/msec^2 acceleration limit. This ensures that only a three-branch power stroke occurs, thus simplifying the computational determination of the optimal trajectory.

B. Optimized piston trajectories

Piston velocity on the power stroke is shown in Fig. 2. Plotted are curves of (i) optimized piston motion with acceleration constraints and (ii) conventional piston motion. Pa-

TABLE II. Parameters for different discussed cases.

Case	Variation from Table I
Std	none
I	$t_b = 0.1$ msec
II	$t_b = 1.0$ msec
III	$t_b = 5.0$ msec
IV	$\tau = 66.66$ msec, corresponding to 1800 rpm
V	$k = 2610$ kg K^{-1} sec^{-3}
VI	$\alpha = 25.8$ kg sec^{-1}

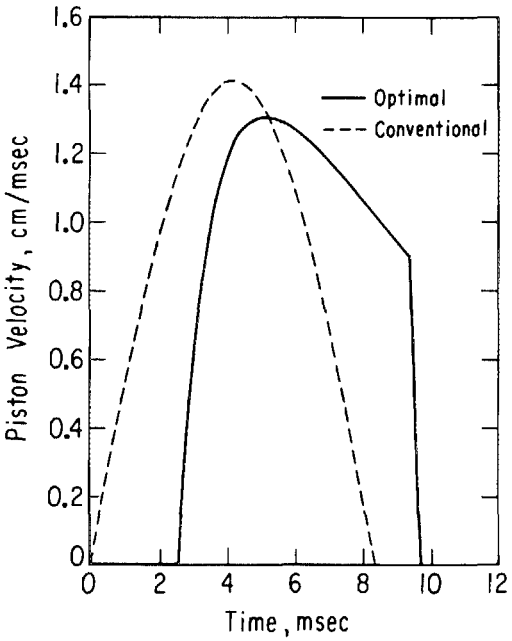

FIG. 2. Comparison of optimal ($|a_{max}| = 3.0$ cm msec^{-2}) and conventional piston velocities on the power stroke for case Std.

rameter values used in this figure are for case Std.

The optimized power stroke begins with a zero-velocity branch. This seemingly bizarre behavior increases losses from heat leakage because the motion delay time t_d increases the maximum temperature of the working fluid. The delayed motion also increases frictional losses because the piston must move the distance Δx in a time less than t_p. However these losses are outweighed by gains in the efficiency: the delayed motion raises the temperature of the working fluid along the power stroke, increasing the maximum availability of the system. In Fig. 3 the temperature profile along the optimal power stroke path is contrasted with the lower temperatures reached along the conventional power stroke. The

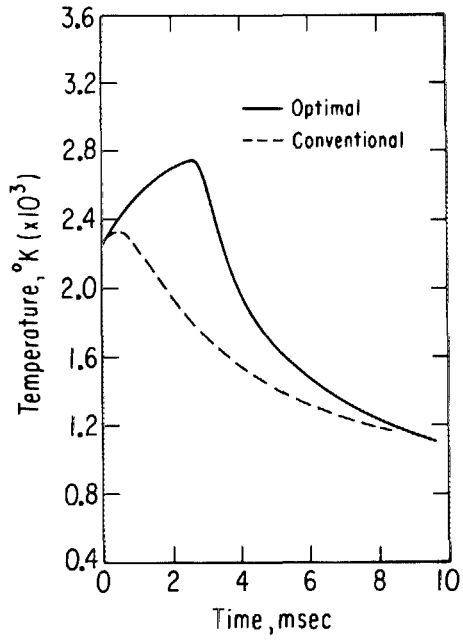

FIG. 3. Comparison of optimal ($|a_{max}| = 3.0$ cm msec^{-2}) and conventional working fluid temperatures on the power stroke for case Std.

TABLE III. Time and temperature results for different cases.

Case	a_{max} (cm msec^{-2})	t_d (msec)	$T(t_d)$ (K)	t_b (msec)	t_p (msec)	t_1 (msec)	t_2 (msec)
Std		2.55	2742	2.50	9.67	6.33	10.97
Std	3.0	2.56	2745	2.50	9.66	6.46	10.72
I		0.20	3173	0.10	5.81	7.37	12.77
II		1.49	2967	1.00	7.68	6.87	11.90
II	3.0	1.50	2951	1.00	7.71	6.98	11.65
III		2.85	2526	5.00	11.33	5.89	10.20
III	3.0	2.95	2527	5.00	11.28	6.04	9.95
IV		2.62	2750	2.50	11.08	14.89	25.79
IV	3.0	2.65	2752	2.50	12.00	14.69	25.25
V		1.30	2516	2.50	8.04	6.77	11.73
V	3.0	1.30	2516	2.50	8.06	6.88	11.48
VI		2.10	2711	2.50	10.07	6.23	10.79
VI	3.0	2.10	2713	2.50	10.01	6.37	10.56

duration of the zero-velocity arcs, the temperatures at the end of these arcs, burn times, and the time spent on each stroke are listed in Table III. Values for the cases of unlimited and limited acceleration differ only slightly.

The zero-velocity arcs are a consequence of the fixed compression ratio of our model. Without this constraint the optimized system would start its power stroke by moving the piston to $x < x_0$ to achieve even higher internal temperatures. This behavior is reminiscent of the work of Band, Kafri, and Salamon,[16] who found that the optimal expansion stroke for their particular heating function was one which at first compressed the gas as the heat input became larger than the initial internal energy of the gas.

The unbounded arcs of the power stroke show a large initial acceleration. The rapid volume increase limits the temperature rise, even though combustion within the cylinder continues. A plot of temperature versus time, as in Fig. 4, shows the temperature declining at its greatest rate immediately following the motion delay time. In this way the system heat-conduction losses which dominate the loss mechanisms in the high-temperature regions are minimized. As the temperature of the working fluid decreases, frictional losses be-

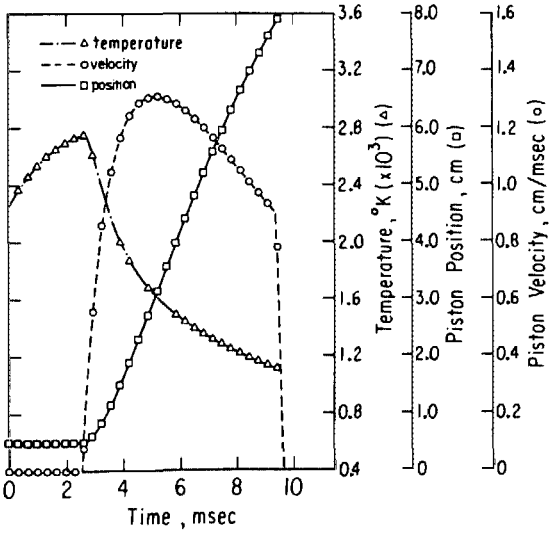

FIG. 4. Working fluid temperature, piston position, and piston velocity along the optimal power stroke for case Std ($|a_{max}| = 3.0$ cm msec^{-2}).

come relatively more important. The piston velocity changes slowly, mimicking the optimal constant velocity trajectory characteristic of the nonpower strokes. However instead of becoming constant, the velocity decreases slowly along the power stroke as heat continues to leak to the environment.

C. Comparison of optimal (Ref. 17) and conventional engine performance

Table IV lists energies which characterize the operation of our optimal and conventional engines. We observe similar qualitative behavior for the cases of unconstrained and constrained acceleration. Losses from friction in the power and nonpower strokes are given under the headings of W_{fP} and W_{fNP}, respectively. Net friction losses, $W_{fP} + W_{fNP}$, are headed by W_f. Heat-leak losses are listed under L_Q. Losses due to dissipating hot exhaust gases into the environment are termed L_{ex1}. Losses due to incomplete combustion are termed L_{ex2}. The work done during the power stroke by the gas as it expands against the piston is given by $W_{P,expan}$. Total work output along the power stroke is $W_{P,expan} - W_{fP}$ and is labeled W_P. The required compressional work input along the optimal compression stroke is given by W_{com}. If we assume an external work reservoir, such as a flywheel, provides W_{com} then total work output over one cycle of our engine is

$$W_{cycle} = W_P - W_{fNP}.$$

This quantity is the objective function that was optimized in Sec. III. If our engine must provide W_{com}, then the optimal net work output per cycle for our engine is

$$W_{net} = W_{cycle} - W_{com}.$$

The connection between these energy terms is clarified by examining the energy balance for the engine. We have

$$U_i + (Q_c - L_{ex2}) + W_{com} = U_f + W_f + L_Q + W_{cycle}, \quad (41)$$

where U_i and U_f are the initial and final internal energies of the contained gas and Q_c is the heat of combustion contained in one fuel charge. Alternately, Eq. (41) may be expressed as

$$C_i N_i T_0 + (Q_c - L_{ex2}) + W_{com} = C_f N_f T_0 + L_{ex1} + L_Q + W_{cycle} + W_f.$$

The subscripts i and f refer to conditions at the beginning and end of the power stroke, respectively. T_0 is the temperature of the environment.

We begin our comparison of optimal and conventional trajectories with case I. The burn time here is very fast compared to the cycle time. This case approaches the Otto cycle limit where complete combustion is assumed to occur instantaneously. Substantial gains in power output are achieved by optimizing the cycle. Heat-leak losses are 22.7% less along the optimal power stroke than along the conventional trajectory. The high velocities necessary to reduce heat-leak losses result in higher friction losses along the optimal power stroke, by comparison with the conventional path. However, these high power-stroke piston velocities result in a longer time interval being allocated to the optimal nonpower strokes. Average velocity is thus smaller along the optimal nonpower strokes, so that the total friction losses are reduced below those of the conventional cycle. Similar results were noted by Mozurkewich and Berry in their path optimization of the Otto cycle.[7]

This behavior changes as the burn time increases. With slower burns, high power-stroke temperatures do not occur. Heat leak in the first part of the power stroke no longer dominates the loss terms. The relative improvements obtained by reducing the heat leak are decreased dramatically. Correspondingly, frictional losses become more important. An examination of cases II, Std, and III illustrates this shift.

Case II, with a 1.0-msec burn time, shows lower relative improvements from the conventional to the optimal power strokes, in both heat-leak and frictional losses. Relative heat-

TABLE IV. Results for optimal and conventional piston cycles (energies in units of joules).

Case	a_{max} (cm msec^{-2})	W_{fP}	W_{fNP}	W_f	L_Q	L_{ex1}	L_{ex2}	$W_{P,expan}$	W_P	W_{com}	W_{cycle}	W_{net}
Std		21.5	42.7	64.2	240.9	332.0	8.6	672.5	651.0	199.6	608.3	408.7
Std	3.0	21.8	44.0	65.8	240.7	332.1	8.6	672.6	650.8	199.6	606.8	407.1
Std	conv	21.5	53.7	75.2	203.1	362.4	14.0	645.8	624.3	199.6	570.6	370.9
I		29.1	36.7	65.8	155.8	357.2	0.0	775.6	746.5	199.6	709.8	510.2
I	conv	21.8	54.6	76.4	214.6	319.2	0.0	755.4	733.6	199.6	679.0	479.4
II		25.1	39.4	64.5	203.5	344.8	1.9	725.6	700.5	199.6	661.1	461.5
II	3.0	25.3	40.5	65.8	204.0	344.0	0.2	725.8	700.5	199.6	660.0	460.4
II	conv	21.8	54.6	76.4	212.9	337.2	0.1	707.6	685.7	199.6	631.2	531.5
III		18.6	46.0	64.6	256.1	310.9	42.6	616.0	597.4	199.6	551.4	351.8
III	3.0	19.0	47.5	66.4	254.7	311.3	42.9	616.0	597.0	199.6	549.6	349.9
III	conv	21.8	54.6	76.4	179.6	347.2	77.8	584.9	563.1	199.6	508.5	308.9
IV		18.5	18.2	36.6	268.0	332.1	8.5	671.1	652.6	199.6	634.5	434.8
IV	3.0	17.3	18.6	35.8	284.1	298.6	3.4	670.4	653.1	199.6	634.6	435.0
IV	conv	10.9	27.3	38.2	346.5	245.4	0.5	653.4	642.5	199.6	615.2	415.6
V		23.0	40.0	63.0	334.2	268.1	15.9	612.4	589.4	199.6	549.4	349.8
V	3.0	23.3	41.1	64.3	334.5	267.6	16.4	612.5	589.2	199.6	548.2	348.5
V	conv	21.8	54.6	76.4	332.2	265.9	14.6	604.0	582.1	199.6	527.6	327.9
VI		38.3	86.9	125.2	246.7	327.8	7.1	670.2	632.0	199.6	545.0	345.4
VI	3.0	39.0	89.4	128.4	245.2	328.5	7.5	670.4	631.4	199.6	541.9	342.3
VI	conv	43.7	109.2	152.8	203.2	363.8	14.6	641.3	597.6	199.6	488.4	288.8

leak losses are reduced only 4.4% along the optimal power stroke as compared to the conventional power stroke; friction losses are 15.1% higher along the optimal path. Total friction losses for the case II optimal cycle are 15.6% below those of the conventional cycle.

The Std case, with a burn time of 2.5 msec, actually exhibits greater heat-leak losses along the optimal path than along the conventional path. Heat-leak losses are 18.6% higher for the optimal path than for the conventional path. A comparison between the heat-leak losses for the optimized and conventional paths is shown in Fig. 5. The oscillating behavior of the heat-leak loss during the conventional motion is due to the rapid expansion that occurs in the middle of the conventional power stroke. The rapid increase in the area of the exposed heat-conducting surface offsets the decelerating temperature decline to cause the second peak in the curve of heat-conduction loss of the conventional power stroke.

Frictional losses for the entire optimal cycle are 13.6% lower than those for the conventional engine. Frictional losses along the power stroke are larger for the optimal path by a scant 1.3% in this case. This behavior stems from the distribution of times along the optimal path. As burning time increases, a larger share of the cycle time is allocated to the power stroke. Heat-leak losses increase and losses from power stroke friction, L_{ex1} and L_{ex2}, decrease for progressively longer power strokes. Reductions in L_{ex1} reflect the lower working fluid temperatures at the end of the power stroke, implying a greater conversion of the system's internal energy into mechanical work.

We summarize the results of cases I, II, Std, and III: increasing burn times shifts the dominant loss mechanism from the heat-leak loss to the exhaust loss. The increased relative improvements in power output with greater burn times comes from extracting more of the internal energy of the exhaust gases.

Doubling the cycle time, as in case IV, effectively reduces the burn time relative to the cycle time. In light of the above discussion it is not surprising that heat-leak losses dominate the limits on the work output along the optimal path. Heat-leak losses are 22.7% lower for the optimal path than for the conventional path. Power-stroke frictional losses are 69.7% higher along the optimal trajectory. The time allocated to the optimal power stroke, while increased, is not double the time spent on the optimal power stroke in the Std case.

Case V illustrates the relative importance of heat leak. As Fig. 6 shows, doubling the heat-transfer coefficient results in a briefer power stroke as the system attempts to reduce heat losses by decreasing the maximum power-stroke temperature. Heat-leak losses are only 0.6% greater along the optimal path than along the conventional trajectory for this case. Frictional losses along the power stroke are 6.9% greater along the optimal path than along the conventional path. Contrast this with case Std where the same losses are greater by 18.6% and 1.3%, respectively, along the optimal power stroke as compared with the conventional power stroke. Also reflecting the increased importance of heat leak in case V are the terms L_{ex1} and L_{ex2}. These terms are greater along the optimal path than along the conventional path. Contrast this with the Std case where the same losses are greater along the conventional path.

Case VI probes engine behavior when frictional losses are stressed. When the friction coefficient is doubled the optimal path is one which increases the time spent on the power stroke in order to reduce the average piston velocity. Also, as frictional losses become greater, the optimal path tends to a more nearly constant velocity stroke (Fig. 7), which is the best path when only frictional losses are present. Frictional losses along the optimal nonpower and power strokes are reduced by 20.4% and 12.6%, respectively, as compared to the conventional piston path. These improvements exceed

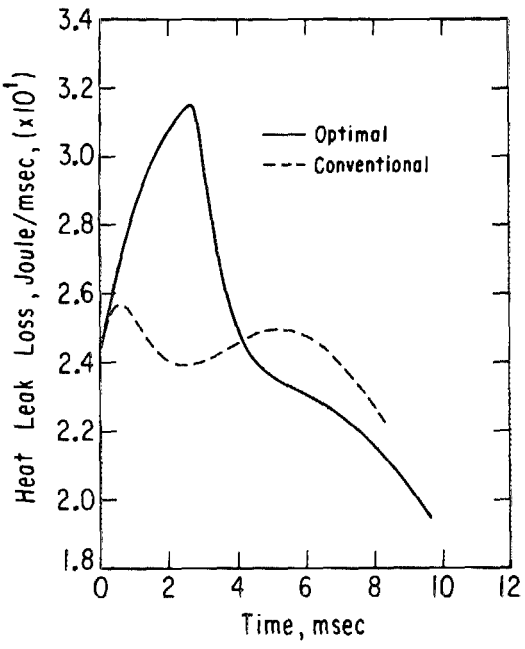

FIG. 5. Comparison of optimal ($|a_{max}| = 3.0$ cm msec^{-2}) and conventional heat losses on the power stroke for case Std.

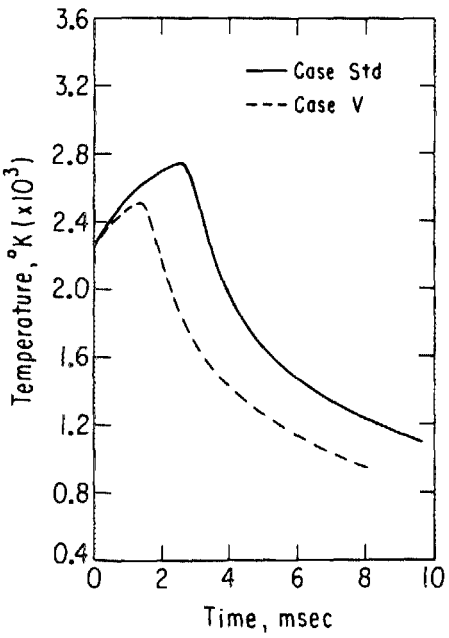

FIG. 6. Working fluid temperature on the optimal power stroke for case Std and case V ($|a_{max}| = 3.0$ cm msec^{-2}).

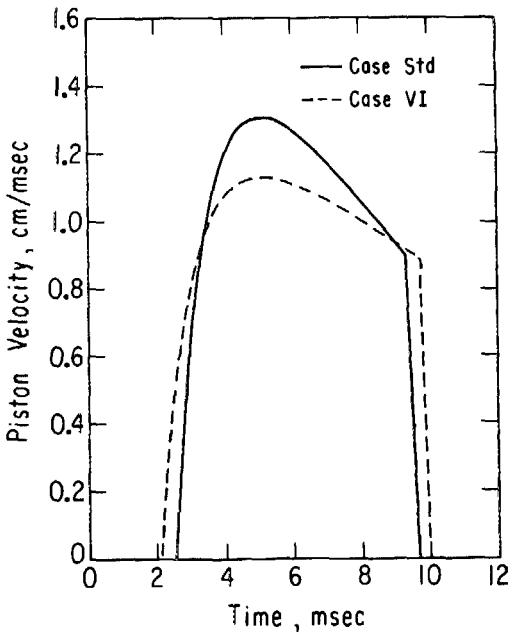

FIG. 7. Piston velocity on the optimal power stroke for case Std and case VI ($|a_{max}| = 3.0$ cm msec^{-2}).

case Std where the optimal trajectory boasts relative reductions in frictional losses of 18.1% along the nonpower strokes and of -1.3% along the power stroke. Heat-leak losses are 21.4% greater along the optimized power stroke relative to the conventional power-stroke motion.

D. Figures of merit

We use the standard figures of merit, net efficiency n_1 and thermal efficiency n_2,[8,18] to present enhancements in engine performance resulting from modifying the conventional piston path. Net efficiency

TABLE V. Results for figures of merit.

Case	a_{max} (cm msec^{-2})	n_1	n_2
Std		0.493	0.571
Std	3.0	0.492	0.571
Std	conv	0.448	0.539
I		0.616	0.696
I	conv	0.579	0.671
II		0.557	0.635
II	3.0	0.556	0.635
II	conv	0.521	0.613
III		0.425	0.503
III	3.0	0.423	0.503
III	conv	0.373	0.465
IV		0.525	0.569
IV	3.0	0.525	0.569
IV	conv	0.502	0.548
V		0.422	0.499
V	3.0	0.421	0.499
V	conv	0.396	0.488
VI		0.417	0.568
VI	3.0	0.413	0.569
VI	conv	0.349	0.533

TABLE VI. Relative improvements in performance for optimal engine cycle.

Case	a_{max} (cm msec^{-2})	$\%\Delta W_{cycle}$	$\%\Delta W_{net}$	$\%\Delta n_1$	$\%\Delta n_2$
Std		6.5	10.0	10.0	6.0
Std	3.0	6.3	9.8	9.8	6.0
I		4.5	6.4	6.4	3.6
II		4.7	6.9	6.9	3.5
II	3.0	4.6	6.7	6.7	3.6
III		8.4	13.9	13.9	8.1
III	3.0	8.1	13.3	13.3	8.1
IV		3.1	4.6	4.6	3.9
IV	3.0	3.1	4.7	4.7	3.7
V		4.1	6.7	6.7	2.1
V	3.0	3.9	6.3	6.3	2.1
VI		11.6	19.6	19.6	6.6
VI	3.0	11.0	18.5	18.5	6.6

$$n_1 = W_{net}/Q_c$$

is a measure of the useful work obtained from the engine. Thermal efficiency

$$n_2 = (W_{P,expan} - W_{com})/Q_c$$

is a measure of the work done by the expanding gas. Table V tabulates the efficiencies obtained for the cases discussed above. Finally, Table VI summarizes the relative improvements in engine performance due to modifying the cycle path to obtain maximum work output per cycle.

ACKNOWLEDGMENTS

This work benefited from helpful conversations with Dr. Michael Mozurkewich. This work was supported by the Division of Basic Energy Sciences of the United States Department of Energy. Additionally, one of us (K. H. H.) would like to thank the Deutsche Forschungsgemeinschaft for supporting this work and the University of Chicago for the hospitality extended during this stay.

[1] B. Andresen, R. S. Berry, A. Nitzan, and P. Salamon, Phys. Rev. A **15**, 2086 (1977).
[2] M. H. Rubin, Phys. Rev. A **19**, 1272 (1979).
[3] M. H. Rubin, Phys. Rev. A **19**, 1277 (1979).
[4] P. Salamon, A. Nitzan, B. Andresen, and R. S. Berry, Phys. Rev. A **21**, 2115 (1980).
[5] P. Salamon and A. Nitzan, J. Chem. Phys. **74**, 3546 (1981).
[6] B. Andresen, P. Salamon, and R. S. Berry, J. Chem. Phys. **66**, 1571 (1977).
[7] M. Mozurkewich and R. S. Berry, J. Appl. Phys. **53**, 34 (1982).
[8] C. F. Taylor, *The Internal Combustion Engine in Theory and Practice* (MIT, Cambridge, Massachusetts, 1966), Vol. I, pp. 135–142.
[9] C. F. Taylor, *The Internal Combustion Engine in Theory and Practice*, Ref. 8, Vol. I, pp. 312–356.
[10] C. F. Taylor, *The Internal Combustion Engine in Theory and Practice*, Ref. 8, Vol. I, p. 333.
[11] C. F. Taylor, *The Internal Combustion Engine in Theory and Practice*, Ref. 8, Vol. I, pp. 123 and 136.
[12] J. C. Hsu and A. U. Meyer, *Modern Control Principles and Applications* (McGraw-Hill, New York, 1968).
[13] A. E. Bryson, Jr. and Y.-C. Ho, *Applied Optimal Control* (Wiley, New

York, 1975).
[14]The program VMCON was graciously provided by M. Minkoff, Argonne National Laboratories, Argonne, Illinois 60439.
[15]C. F. Taylor, *The Internal Combustion Engine in Theory and Practice*, Ref. 8, Vol. II, pp. 439 and 463.
[16]Y. B. Band, O. Kafri, and P. Salamon, Chem. Phys. Lett. 7, 127 (1980).
[17]Unless explicitly stated the comparisons are taken between the optimal path for the constrained acceleration case and the conventional path.
[18]T. D. Eastop and A. McConkey, *Applied Thermodynamics for Engineering Technologies* (Longman Group, Singapore, 1981).